Hot Deformation Behavior of Ti-6Al-4V Alloy in α and α+β Phase Field

TZE-CHING YANG, HSIAO-TZU CHANG, CHAO-HSIEN WU, IN-TING HONG and YEONG-TSUEN PAN

New Materials Research & Development Department
China Steel Corporation

The microstructure evolution during hot deformation was investigated for Ti-6Al-4V alloy with initial acicular and lamellar microstructure. The Ti-6Al-4V alloy was deformed at the temperatures of 900℃ and 780℃ with the strain rates of 1s^{-1}, 10 s^{-1} and 50s^{-1} by a uni-axial deformation machine, respectively. The Ti-6Al-4V alloy deformed at α+β phase field temperature followed by the β solution heat treatment which exhibited the apparent work-hardening characteristics, while that deformed at a lower (α phase field) temperature following the α+β solution heat treatment, which exhibited the predominantly dynamic recovery and dynamic recrystallization-assisted softening behavior. The finer microstructure of β solution treated specimen can be obtained using a rolling route with higher strain rate at α+β and α phase field temperature, thus leading to better mechanical properties.

Keywords: Hot deformation behavior, Ti-6Al-4V alloy, Work-hardening, Recovery and recrystallization

1. INTRODUCTION

Titanium is an important engineering material and widely used in the aviation and aerospace industries because of its low density, high strength, toughness and good high temperature properties(1-3). The desired strength feature and corrosion resistance are achieved by the accurate control of deformation route and microstructure. To obtain the desired microstructure of Ti-6Al-4V titanium alloy, plastic deformation coupled with phase transformation, such as work hardening, dynamic recovery, and dynamic recrystallization, in the α+β↔β phase transformation range with proper conditions is essential(4). Grain refinement can be achieved by preliminary heat treatment in the thermo-mechanical process. Final heat treatment operations are usually used for the stabilization of microstructure(5). The previous researchers have tried to investigate the microstructure and mechanical characteristics during hot working in the α+β phase region. However, few researches have been devoted enough to analyze the hot deformation behavior in the β-phase region and explored the effect of the occurrence of the Dynamic Recrystallization (DRX)(4). Although a lot of literature is available on hot working behavior of this alloy, very little attention has been paid to correlate hot rolling conditions to the mechanical properties(6). In addition, limited data on the effect of actual rolling conditions on tensile properties are available. Consequently, the purpose of the study was to investigate the relationship between the thermomechanical processing parameters and the microstructure and corresponding tensile property by using the hot deformation simulator and the on-line hot rolled mill.

2. EXPERIMENTAL METHOD

The composition of Ti-6Al-4V alloy was listed in Table 1, which was received as a hot rolled plate with a 4mm thickness. The beta transformation temperature is measured to be approximately 1032°C by thermal dilatometer method as shown in Fig.1(a). The as-received material was primarily subjected to beta solution treatment at 1100°C for 3mins followed by a slow cooling rate of 0.1°C/s. Figure 1(b) shows the microstructure is

Table 1 The chemical composition of Ti-6Al-4V alloy

Element	Al	V	Fe	C	N_2	O_2	H
wt%	6.3	4.1	0.16	0.02	0.005	0.11	0.002

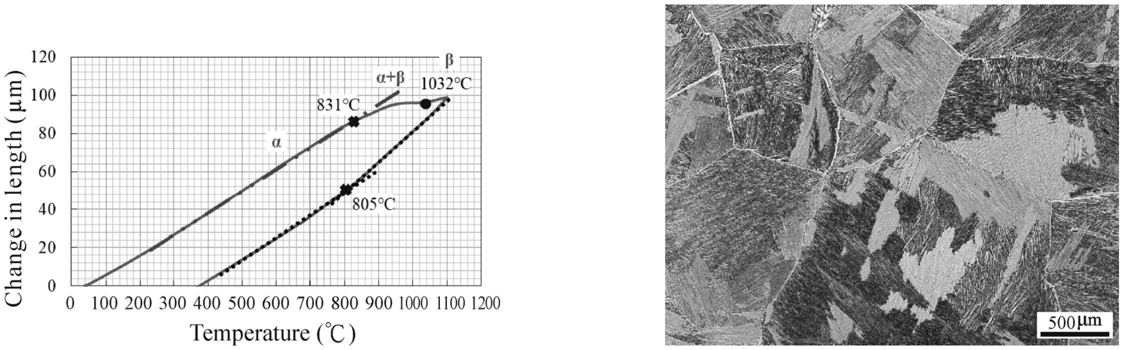

(a) (b)

Fig.1. (a) The CCT curve and (b) initial microstructure of Ti-6Al-4V alloy.

consisted of a lamellar α within the prior β grains along with grain boundary α. The grain size was measured to be about 560μm. The deformation samples with dimensions of 10mm in height and 5mm in diameter were sectioned along the transverse rolling direction of the as-received plate. An DIL 805 A/D dilatometer testing machine equipped with a fully digital and computerized control furnace was employed to perform hot deformation tests under constant strain rates with $1s^{-1}$, $10s^{-1}$ and $50s^{-1}$ at interval of an order of magnitude and at temperature of 780 and 900°C. Various rolling routes such as the α+β two-phase region rolling (rolling at a temperature range between 800°C and 930°C, and the single beta phase region rolling(rolling at the temperature of 1050°C); with a rolling strain rate of $10s^{-1}$ and a total reduction of 95% performed in thirteen-passes were designed. All plates were air cooled after rolling and then prepared according to the standard procedures and subjected to microstructure observations by optical microscopy and tensile testing.

3. RESULTS AND DISCUSSION

3.1 Microstructure of solution treated specimens

Figure 2 shows the microstructures of specimens subjected to β and α+β solution treatment, respectively. It can be found that the finer acicular α phase and the continuous α phase on the prior β boundary in the β-solution treated specimen as shown in Fig.2(a), while an α-β lamellar structure with α-phase lamellae in a β-phase matrix in the α+β-solution treated specimen as shown in Fig.2(b). It is well known that the formation of α-lamellae is a diffusion controlled nucleation and growth process.

3.2 Effect of deformation temperature

The deformation behavior of β and α+β solution treated specimens after the large reduction in α+β and α region are illustrated in Fig.3. All the deformed curves exhibit stress increases with initial increasing strain up to a peak stress then decreases with further strain. The softening after peak stress is well recognized to be attributed from the occurrence of dynamic globularization and deformation heat. In this paper, the softening contributed from deformation heat is neglected. It was found that the peak stress of specimens subjected to the β and α+β solution treatment performed opposite

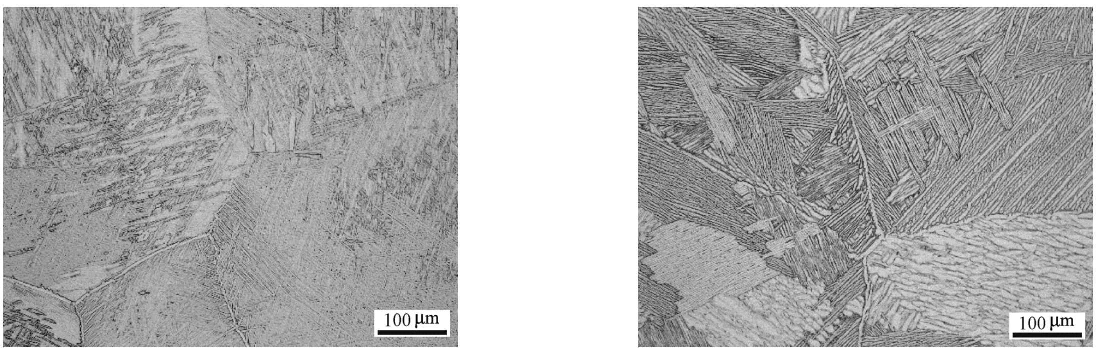

(a) (b)

Fig.2. Microstructure of as-received specimens subject to (a) β and (b) α+β solution treatment and air cooling at a rate of around 5°C/s.

results at 780°C and 900°C deformation temperature, respectively. The β solution treated specimen deformed at 900°C showing a lower peak stress and larger critical dynamic globularization strain compared with that of the specimen when it was deformed at 780°C. In contrast, the α+β solution treated specimen deformed at 900°C showing a lower peak stress and smaller critical dynamic globularization strain compared with that of the specimen when it was deformed at 780°C. It was also found that the β solution treated specimen exhibited lower peak stress than that of the α+β solution treated specimen when they were deformed at 900°C. In contrast, the β solution treated specimen exhibited higher peak stress than that of the α+β solution treated specimen when they were deformed at 780°C.

Figure 4 shows the microstructures of the α+β (950°C) and β (1050°C) solution treated samples after one pass for 50% total reduction through the 10 s^{-1} strain rate at 780°C. It was found that the elongated α grains were more distinct, and the aspect ratio of the alpha grain size decreases when the solution temperature was raised from 950°C to 1050°C. However, the higher deformation temperature, especially on α+β (900°C) phase field, leads to enlarge lamellar width after the β solution treatment, as shown in Fig.5. It suggests that the β solution treatment is the key factor to obtain a greater amount of fine acicular α phase, and the fine grained structure can be achieved via the deformation in α phase field temperature. Comparing Fig.4

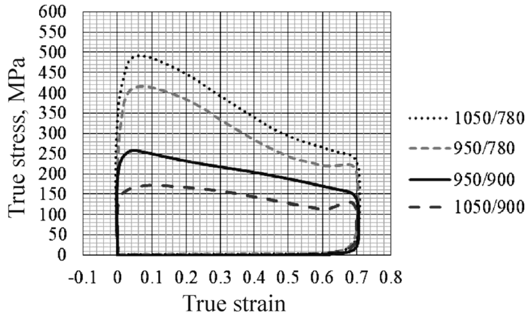

Fig.3. True stress-true strain curve of the α+β (950°C) and β (1050°C) solution treated samples after one pass for 50% total reduction through the $10s^{-1}$ strain rate at 780°C and 900°C.

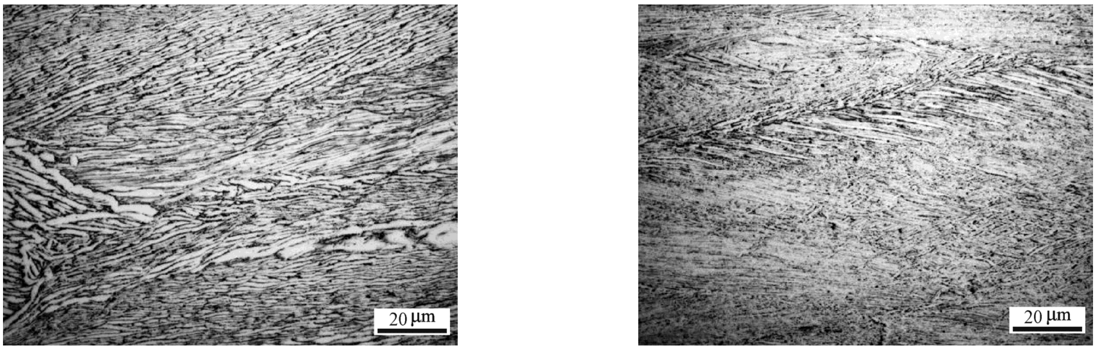

(a) (b)

Fig.4. Microstructures of the (a) α+β (950°C) and (b) β (1050°C) solution treated samples after one pass for 50% total reduction through the $10s^{-1}$ strain rate at 780°C.

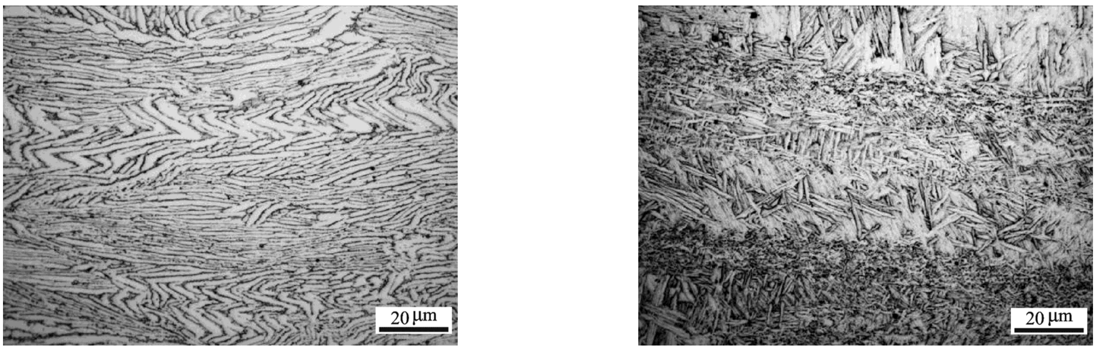

(a) (b)

Fig.5. Microstructures of the samples the (a) α+β (950°C) and (b) β (1050°C) solution samples after one pass for 50% total reduction through the $10s^{-1}$ strain rate at 900°C.

with Fig.3, it was found that the deformation effect gives rise to more globularization of partially globularized α grains, which was apparent when a higher deformation temperature was applied.

3.3 Strain rate effect

The true stress-true strain curves from deformation at strain rates of $1s^{-1}$, $10s^{-1}$ and $50s^{-1}$ and deformation temperatures of 780°C and 900°C are illustrated in Fig.6 and the peak stresses are listed in Table 2. No matter what strain rate of the β(1050°C) or α+β(950°C) solution treated specimens passed through, the peak stress increased with strain rate at a given deformation temperature. The α+β solution treated specimens showed flow softening for all three strain rates. At the low deformation temperature (780°C), the specimen subjected to a medium high strain rate ($10s^{-1}$) revealed a significant stress drop with increasing strain (up to the true strain of 0.36), and then the true stress increased with increasing strain. For the β solution treated condition, the flow stress increases with increasing strain then reaches a plateau at the higher deformation temperature, but the flow curves exhibit the decreasing trend at the lower deformation temperature. It was noted that associated with the highest strain rate ($50s^{-1}$), the true strain would spring back to 0.025 before peak stress, and then extended the long strain to 0.64 during the lower temperature deformation for both α+β and β solution treated specimens.

For the β solution treated samples, the optical micrographs of the isothermal compressed Ti-6Al-4V alloy at a deformation temperature of 900°C and 780°C with the strain rates of 1, 10 and $50s^{-1}$, are shown in Fig.7. The lamellar α phase width of Ti-6Al-4V alloy decrease with increasing strain rate. The grain size and volume fraction of the primary α phase decreased significantly with increasing strain rate. The grain size of the primary α phase in the isothermal compressed Ti-6Al-4V alloy at a strain rate of $1s^{-1}$ as shown in Fig.7(a) is about 120μm, which is obviously larger than that at the higher strain rates, as shown in Fig.7(b). In addition, the strain rate also affects the morphology of the primary α phase in the isothermally compressed Ti-6Al-4V alloy. The morphology of all primary α grain in the isothermal compressed Ti-6Al-4V alloy at a lower strain rate predominantly consists of a small amount of equiaxed α grains and some plate-like α grains. In contrast, some of the fiber-like grains appear at the highest strain rate, as shown in Fig.7(c). Figure 7(d)-(f) show the grain size and lamellar width

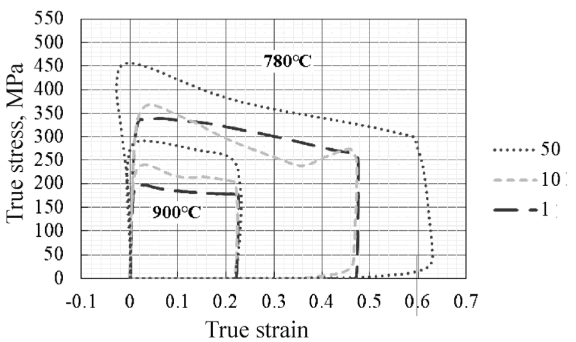

(a)

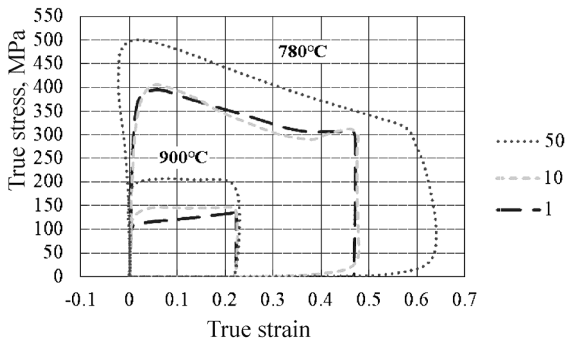

(b)

Fig.6. True stress-true strain curve of the (a) α+β and (b) β solution samples after two pass for the 50% total reduction through the strain rate of $1s^{-1}$, $10s^{-1}$ and $50s^{-1}$

Table 2 The peak stress of Ti-6Al-4V alloy after different deformation parameters

Strain rate \ Temperature	780°C (α+β)	900°C (α+β)	780°C (β)	900°C (β)
$1s^{-1}$	338	196	395	135
$10s^{-1}$	368	240	405	147
$50s^{-1}$	456	291	500	207

*Note: The unit of peak stress: MPa

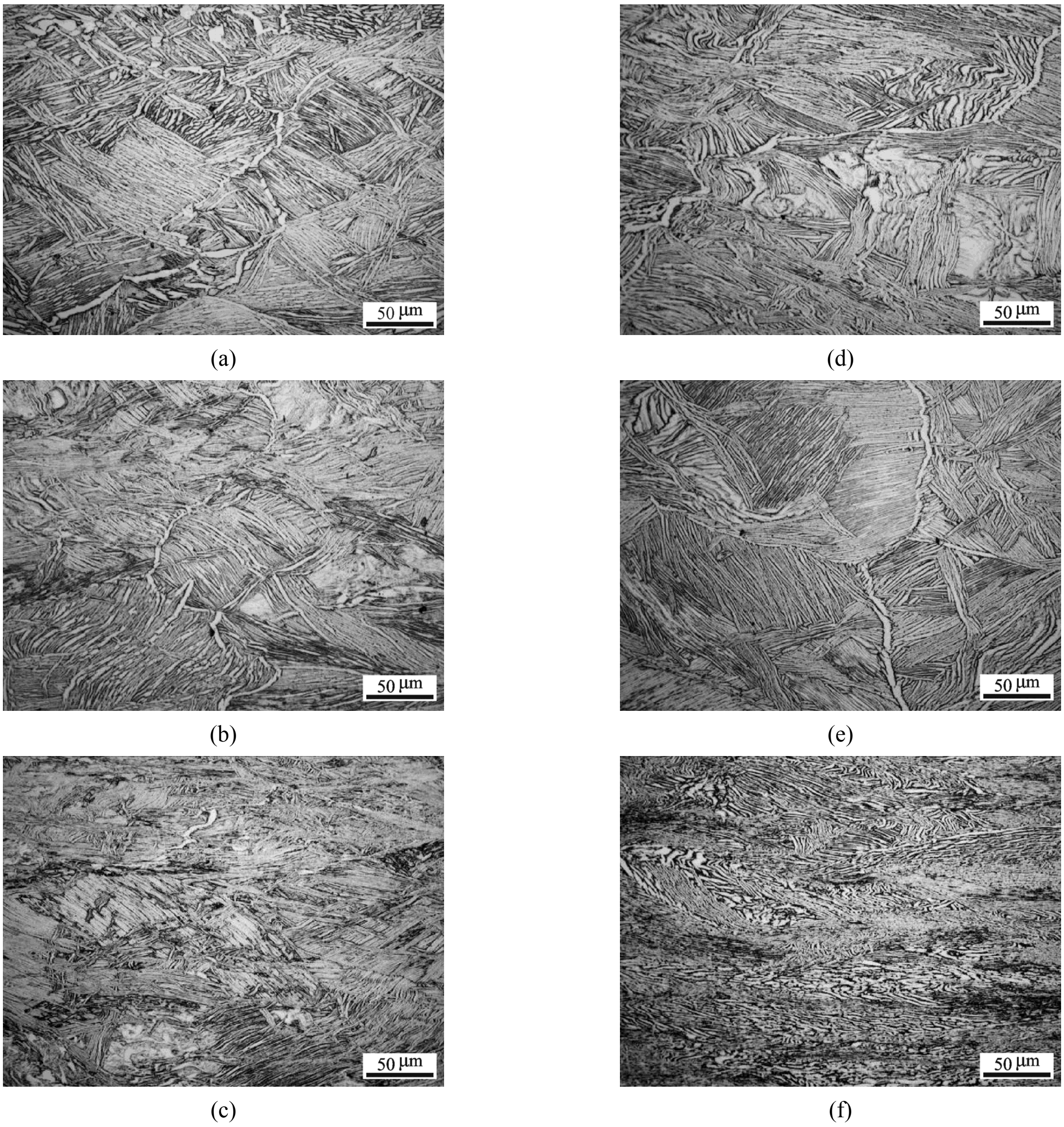

Fig.7. Microstructures of two solution treated samples after the 50% reduction through the three strain rate (a) β-1s^{-1}, (b) β-10s^{-1} , (c) β-50s^{-1}, (d) α+β-1s^{-1}, (e) α+β-10s^{-1} and (f) α+β-50s^{-1}

of primary α were decreased with increasing the strain rate. Otherwise, in the α+β solution treated samples, the primary α grain still possesses the plate-like morphology due to an insufficient driving force for generating the dynamic recrystallization. Since the highest strain rate resulted in the higher dislocation density, the amount of plate grain was reduced and gave rise to a partially globularized α structure in the specimen deformed at the highest strain rate, as shown in Fig.7(f).

3.4 Microstructure and Mechanical properties of Ti-6Al-4V plate

To implement the above deformation simulation results to a Ti-6Al-4V thin plate rolling, the rolling was carried out in between 780°C and 900°C to promote the dynamic recrystallization and crush the plate-like or lamellar α structure. Figure 8 demonstrates the microstructures of the β and α+β solution treated plates through the thermal-mechanical rolling process. All microstructures were characterized as elongated α grains with small amount of equiaxed grains. But, the α+β solution treated plate is mainly consisted of the large equiaxed grain with a small grain mixed structure.

The microstructure of the real rolling plate is significantly different compared with that of the deformation simulation. Such a difference is contributed from a larger total reduction (95.6%) when applied in the real plate rolling to that as applied in the simulation deformation. In addition to grain refinement, a lot of defects, such as dislocations, were induced in to the microstructure of rolled plate, as shown in Fig.9. Subsequently, an annealing process was applied to eliminate the dislocation defects.

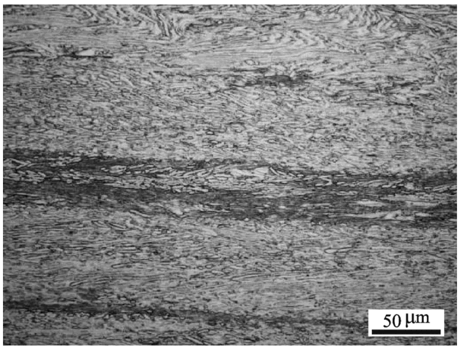

(a)

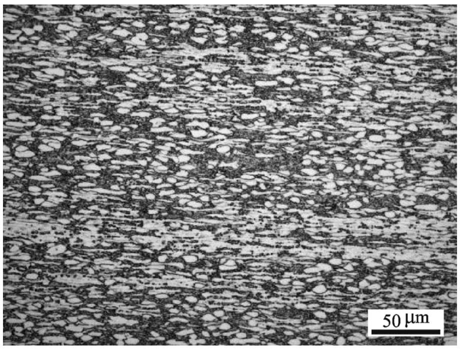

(b)

Fig.8. Optical microscope of the (a) β and (b) α+β solution plate after the rolling procedure

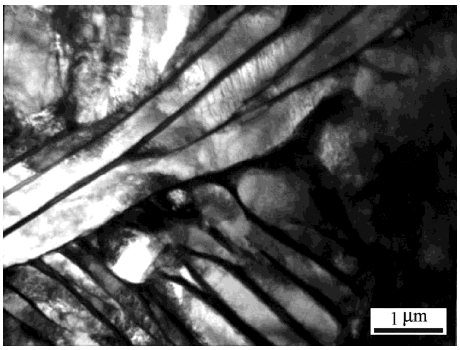

Fig.9. TEM microscope of the β solution treated plate after the rolling

The as-rolled plate without annealing substantially reduces the ductility, due to the presence of the abundant dislocations. However, Fig.10 shows that the tensile behavior of β solution treated plate is similar to that of the α+β solution treated plate, even the microstructure was remarkably different. It was found that the Yield Strength (YS) and Tensile Strength (TS) of Ti-6Al-4V alloy plate decreases with increasing the annealing temperature, while the Elongation (EL) is opposite. The strength and elongation distribution of β solution treated plate with annealing at 700°C for a 2 hour holding period, exhibits better mechanical property performance, which is related to the shorter moving distance of dislocations. Figure 11(a) exhibits the β solution treated plate features a smaller travel distance between the α grain boundary than that in the α+β solution treated plate as shown in Fig.11(b). Therefore, the α+β solution plate needs more thermal energy to drive the motion of dislocation and the occurrence of recrystallization. In accordance with ASTM B265 regulation, the yield strength and tensile strength of Ti-6Al-4V sheet must be greater than 828MPa and 895MPa, hence the plate rolling should apply the structure-controlled deformation schedule developed by this study and meet the regulation.

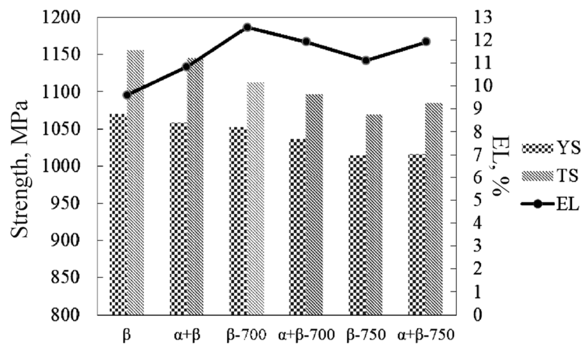

(a)

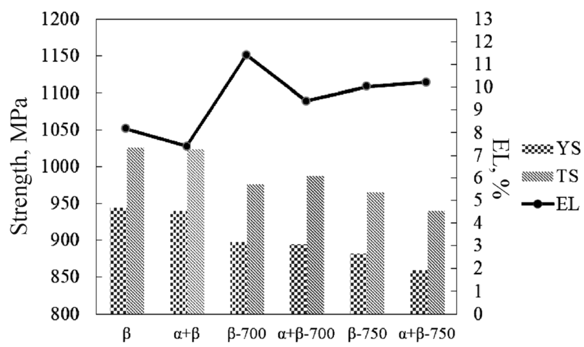

(b)

Fig.10. Tensile properties of Ti-6Al-4V sheet after different annealing temperature for (a) T-direction and (b) L-direction

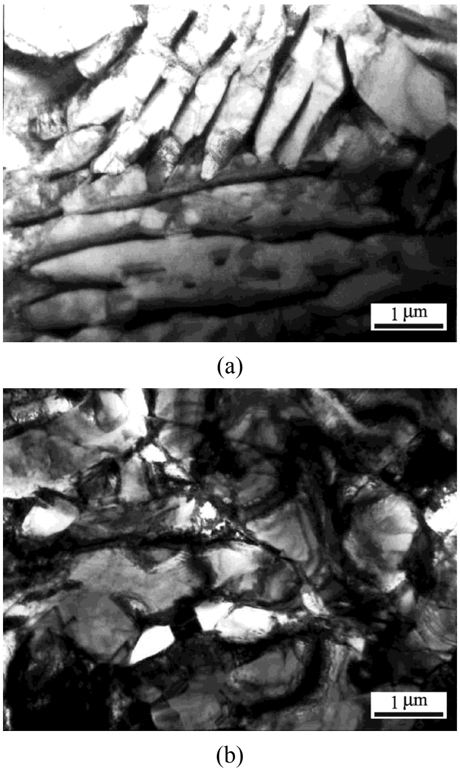

Fig.11. TEM microscope of the (a) β and (b) α+β solution plate after the 700°C/2hrs treatment

4. CONCLUSIONS

1. The microstructure of the un-deformed β solution treated specimen is composed of the finer acicular α phase and the continuous α phase on the prior β boundary, while that of the α+β solution treated specimen is consisted of an α-β lamellar structure with α-phase lamellae in a β-phase matrix.
2. The main deformation characteristic of Ti-6Al-4V alloy was affected by strain rate; which significantly determined the width of lamellar α-phase. Therefore, the grain size and volume fraction of the primary α phase were reduced with increasing strain rate.
3. During hot deformation in the two-phase (α+β) and single-phase (α) regions after β solution treatment, the low strain value applied in each pass and concurrent deformation especially at higher temperatures decelerated the progress of dynamic globularization.
4. Highest deformation strain rate significantly promoted the dynamic globularization and thus refining and smashing the α-phase.
5. The hot rolled plates solution treated in single phase (β) or two-phase (α+β) region exhibited almost the same yield strength, tensile strength and elongation. Nevertheless, the β solution treated plate can be annealed to be a dislocation free structure using a lower annealing temperature due to a smaller dislocation moving distance.

REFERENCES

1. J.C. Williams and E.A. Starke-Jr, Progress in structural materials for aerospace systems, Acta Mater., 2003, Vol. 51, No.19, pp. 5775-5799.
2. S.L. Semiatin, M.W. Corbett, P.N. Fagin, G.A. Salishchev and C.S. Lee, Dynamic-coarsening behavior of an α/β titanium alloy, Metall. Mater. Trans. A, 2006, Vol. 37, No. 4, pp. 1125-1136.
3. S.D. Sun, B. Guo, D.B. Shan and Y. Y. Zhong, Research on elevated temperature deformation behavior of Ti-6Al-4V sheets, Rare Met., 2009, Vol. 28, No. 6, pp. 550-553.
4. R. Ding, Z.X. Guo and A. Wilson, Microstructure evolution of a Ti-6Al-4V alloy during thermomechanical processing, Materials Science and Engineering, 2002, A327, pp. 233-245.
5. M. Motyka and J. Sieniawski, The influence of initial plastic deformation on microstructure and hot plasticity of α+β titanium alloy, Archives of Materials Science and Engineering, 2010, Vol. 41, No. 2, pp. 95-103.
6. A. A. Salem, M. G. Glavicic and S. L. Semiatin, The effect of preheat temperature and inter-pass solution on microstructure and texture during hot rolling of Ti-6Al-4V, Materials Science and Engineering, 2008, A496, pp. 169-176. □